Green and Sustainable Chemistry, 2012, 2, 91-96
http://dx.doi.org/10.4236/gsc.2012.23014 Published Online August 2012 (http://www.SciRP.org/journal/gsc)

Production of Carbon Nanotubes and Hydrogen Catalyzed with Ni/MCM-41 Catalysts

Zhiqi Wang[1*], Juan Navarrete[2]
[1]The American School Foundation, Mexico City, Mexico
[2]Dirección de Investigación y Posgrado, Instituto Mexicano del Petróleo, Mexico City, Mexico
Email: [*]wang_extreme@hotmail.com

Received March 27, 2012; revised April 28, 2012; accepted May 21, 2012

ABSTRACT

Methane catalytic decomposition (MCD) over Ni/MCM-41 catalysts was tested in a microreactor to simultaneously produce hydrogen and carbon nanotubes (CNTs). The methane conversion reached 30% to 47% at a moderate temperature range from 400˚C to 600˚C and the catalytic activity of the catalysts remains stable during 500 min steam on time. CNTs were chiefly formed through tip-growth mode, due to the weak interaction between the metallic Ni and the support. Most of the Ni particles are located on the tip of the produced CNTs, which avoids rapid deactivation of the catalyst resulted from carbon encapsulation. Large Ni particles usually lead to the formation of CNTs with big diameter. During the reaction, the shape of Ni particles changed from pseudo-sphere to diamond-like. All the CNTs consist of multiple layer walls and are curved in certain degree.

Keywords: Methane Catalytic Decomposition; Hydrogen, Carbon Nanotubes; Catalysts; Ni/MCM-41

1. Introduction

Currently, a great attention has been paid to the use of hydrogen on a very large scale in chemicals, food and petroleum refining industries, fuel cell technology, space exploration and other fields. Hydrogen as a fuel has several advantages: it is widely available, easy to handle and has the largest heating coefficient among fuels; more important is that, water is the sole product of hydrogen combustion; therefore, it is an environmentally friendly fuels [1,2].

Several techniques have been developed for hydrogen production including: steam reforming, biomass gasification, and water electrolysis etc. [3]. In the steam reforming of hydrocarbons, one of the products, CO, has to be removed by subsequent steps because it strongly poisons the Pt-catalyst which is the key of fuel cell technology. This significantly increases the production cost. Electrolysis of water may offer clean hydrogen without CO; however, it is too expensive as a result of electricity utilization. One of the most promising routes for hydrogen production is the direct decomposition of methane, which has the highest hydrogen to carbon ratio in comparison with other hydrocarbon compounds. Through this approach, formation of CO can be avoided; thus, the subsequent steps for removal of CO are not necessary. This route is believed to be superior to both electrolysis of water and steam reforming from the economical point of view [3,4].

On the other hand, carbon nanotubes have also attracted great attention for a long time due to their excellent properties and potential utilization in a variety of nanotechnologies [5,6]. One technique used to produce CNTs is the catalytic growth of carbon atoms from decomposition of hydrocarbons. In the methane catalytic decomposition (MCD), if the production of both hydrogen and carbon nanotubes can be effectively combined, we may simultaneously obtain CO-free hydrogen and CNTs by using the same reaction.

The most commonly catalysts used for MCD are the transition metals group VIII (Co, Ni or Fe) supported on oxides like Al_2O_3 and SiO_2. Rahammad and coworkers report that the MCD reaction over a 5 wt% Ni/γ-Al_2O_3 showed a high activity between 500˚C and 550˚C in a thermal balance evaluation system [7]. The catalyst exhibited high activity at 500˚C in fifteen hours of reaction. It was rapidly deactivated within 2 - 3 hrs above 600˚C due to the deposition of carbon materials. Carbon formation was also investigated in the MDC over bare α-Fe and with Fe/Al_2O_3, Fe/ZrO_2, Fe/SiO_2 and Fe/TiO_2 catalysts at temperatures between 400˚C and 600˚C [8]. Under the same reaction condition, 13.5 g, 14 g, 17.4 g and 45 g carbon were yielded over the ZrO_2, Al_2O_3, TiO_2 and SiO_2 supported Fe catalysts, respectively. This work

[*]Corresponding author.

clearly shows that catalyst support greatly impacts on the catalytic activity and carbon production.

It is noteworthy that mesoporous materials like MCM-41 and SBA-15 were frequently used as catalyst support due to their great surface area (>800 m^2/g), large pore volume (>0.5 cm^3/g) and ordered pore system [9-11]. Investigating of the catalyst with new support like mesoporous MCM-41 for simultaneous production of CO-free hydrogen and CNTs will be an interesting research task.

In the present work, Ni/MCM-41 catalysts was used for simultaneous production of CO-free hydrogen and CNTs and its catalytic activity and stability were tested in a microreactor using methane as reaction feedstock. Carbon nanotube formation, including its wall thickness, length, diameter and shape was discussed.

2. Experimental

2.1. MCM-41 Synthesis

For MCM-41 synthesis, fumed silica was used as Si source and cetyltrimethylammonium chloride (CTACl) as synthetic template. 1.2 g of fumed silica were added into 10.0 g of 45% tetrabutylammonium hydroxide (TBAOH) aqueous solution while vigorously stirring for 30 min to form a transparent gel. Then, 30 g of cetyltrimethylammonium chloride (25 wt% solution in water) were added into the above gel during agitation. The gel was thermally aged at 80˚C for 72 h; afterwards, the mixture was filtered and washed 3 times using 500 ml deionized water, and the resultant solid was dried at ambient temperature for 12 hrs. It was then calcined at 600˚C for 6 hrs under an air flow condition (air flow rate was 60 ml/min). In the calcination procedure, care was taken by increasing the temperature with a rate 1˚C/min, in order to avoid mesostructure collapsing of the sample. All the chemicals used in this work were supplied by Sigma Chemical Co. Ltd.

2.2. Preparation of Ni/MCM-41 Catalysts

The Ni/MCM-41 catalysts were prepared by impregnating MCM-41 support with $Ni(NO_3)_2$ solution. The Ni loading of the catalysts was 10 wt%, 20 wt% and 30 wt%, respectively. After impregnation, the Ni supported MCM-41 samples were dried at 70˚C for 10 h and then calcined at 600˚C for 4 h. Before the catalytic evaluation, the catalyst samples were reduced using 99.9% H_2 at 500˚C for 2 h with a flow rate of 30 ml/min to obtain metallic Ni particles on the catalyst.

2.3. Characterization of the Materials

The crystalline structures of the catalyst samples were analyzed with X-ray diffraction technique in a PANalytical difractometer (Model: X'Pert PRD) with a monochromatic Cu$K\alpha_1$ radiation (λ = 1.5400 Å). The evaluation of the diffractograms was made by DIFFRAC/AT software. The scanning was made from 30˚ to 100˚, with a 2θ step size of 0.01˚ and a step time of 2 s.

The Raman spectrum was obtained at room temperature using a LabRam HR 800 spectrometer, equipped with a CCD detector. A laser diode of He-Ne system supplies a 633 nm exciting line and spectral resolution of 4 cm^{-1}.

Transmission electron microscopy (TEM) observations were carried out in a JEM-2200FS transmission electron microscope with accelerating voltage of 200 kV. The microscope was equipped with a Schottky-type field emission gun and an ultra-high-resolution (UHR) configuration (Cs = 0.5 mm; Cc = 1.1 mm; point-to-point resolution, 0.19 nm) and an omega-type in-column energy filter. The powder samples were grounded softly in an agate mortar and dispersed in isopropyl alcohol in an ultrasonic bath for several minutes. A few drops were then deposited on 200 mesh copper grids covered with a carbon film.

2.4. Catalytic Evaluation

The MCD reaction was carried out in a microreactor system (Advanced Scientific Design-RXM-100) with a stainless steel fixed bed reactor (10 mm i.d. and 500 mm in length) at atmospheric pressure. The reaction temperatures varied from 400˚C to 600˚C. The catalyst loading was ca. 150 mg. The inlet mixture was methane diluted in argon. The total inlet flow of the reaction gases was 75 ml/min (6 ml of methane and 69 ml of Ar). The rate of methane fed to the reactor was 2.67 mmol/min. The temperature increasing rate was 10˚C/min. The compositions of the effluents were analyzed by an on-line gas chromatograph (GC) analyzer in couple with a PE-Molsieve capillary column, using a thermal conductivity detector (TCD) for hydrogen analysis and a flame ionization detector (FID) for methane analysis.

3. Results and Discussion

3.1. Structure of Ni/MCM-41 Catalysts

The crystalline structures and phases of the Ni/MCM-41 catalysts were analyzed by XRD technique. As shown in **Figure 1**, several XRD peaks at 44.5˚, 51.5˚, 76.3˚ and 92.7˚ corresponding to metallic Ni in the catalysts are observed. The peak becomes sharper as the Ni loading increases from 10 wt% to 20 wt% and 30 wt%, indicating that the diameter of Ni particle is larger at higher Ni loading.

The morphological features of the Ni/MCM-41 solids were studied by TEM. **Figure 2** shows the TEM micrographs of the 30% Ni/MCM-41 solid calcined at 600˚C.

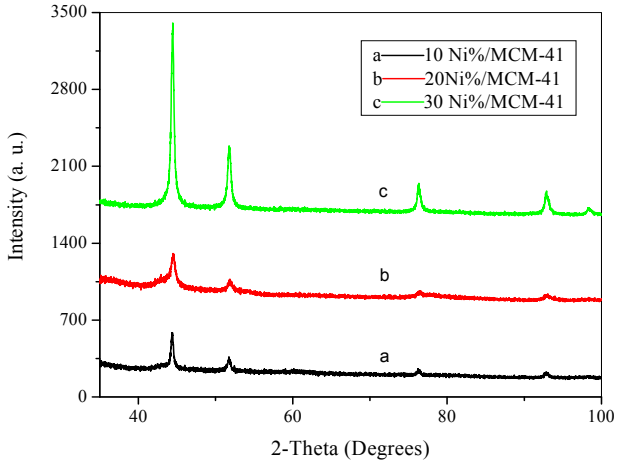

Figure 1. XRD patterns of the catalysts with different Ni content.

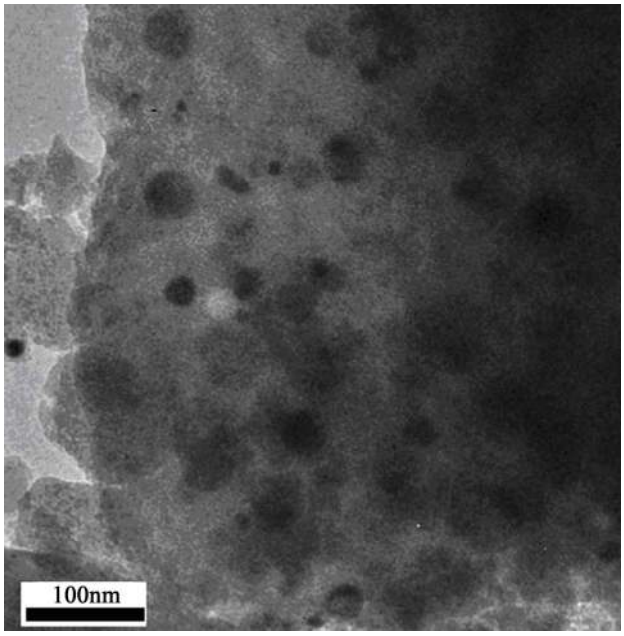

Figure 2. A TEM micrograph of a 30% Ni/MCM-41 catalyst.

In this catalyst, many Ni particles with a shape as pseudo-sphere are observed. The distribution of Ni particle size is not homogeneous, ranging from 10 nm to 50 nm with an average diameter approximately 35 nm. Because the Ni particles were loaded on the catalyst by using an impregnation method, it was difficult to control the Ni particle size distribution; however, the uneven distribution of the Ni particle size allowed us to investigate the effect of Ni particle size on the formation of carbon nanotubes during the reaction.

3.2. Catalytic Evaluation

Methane conversion over the Ni/MCM41catalysts is shown in **Figure 3**. Over all the catalysts, methane conversion increases with the reaction temperature increasing; for example, as the reaction temperature increases from 400˚C to 600˚C, the CH_4 conversion over the 20 wt% Ni/MCM-41 catalyst enhances from approximately 30% to 42%. It is seen that 550˚C is the best reaction temperature. Higher reaction temperature may result in the Ni particles sintering, thus reducing the catalytic activity. In the following experiments, we fixed the reaction temperature at 550˚C.

In order to evaluate the catalytic stability of the catalysts, MCD reaction was also tested in a period of 500 min at 550˚C. The results are presented in **Figure 4**. These catalysts exhibit high stability in this period. The average methane conversion is around 31% for 10% Ni/MCM-41, 43.2% for 20% Ni/MCM-41 and 45.9% for 30% Ni/MCM-41, respectively. It is found that the methane conversion over the 10 wt% Ni/MCM-41 catalyst slightly decreases after 330 min of reaction, an approximately 7% drop is achieved. This catalyst contains small Ni particles which can be easily encapsulated by carbon deposits in the reaction, leading to activity decrease.

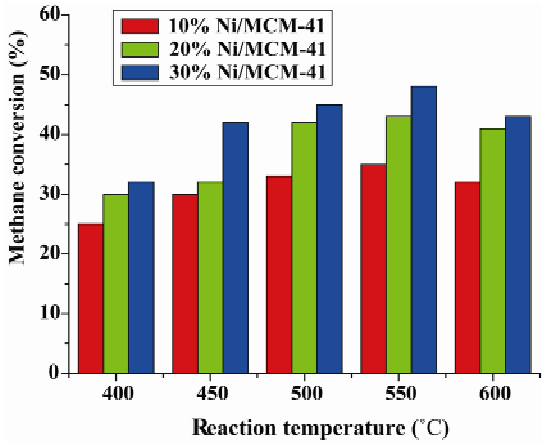

Figure 3. Methane conversion as a function of reaction temperature.

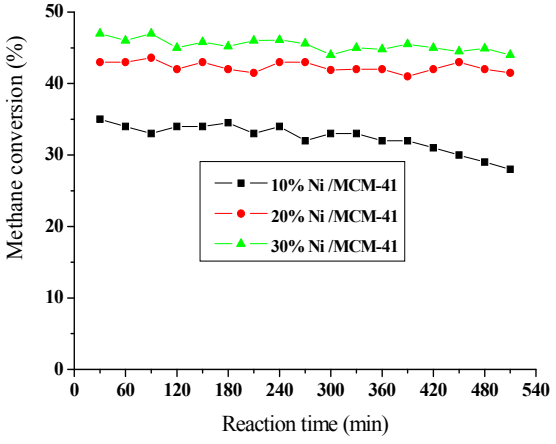

Figure 4. Methane conversion as a function of reaction time.

During the reaction, both CO and CO_2 were not detected. Therefore, hydrogen selectivity was 100%. In 500 min of reaction, around 827 ml, 1146 ml and 1201 ml of hydrogen were respectively produced on the catalysts with 10, 20 and 30 wt% of Ni. The catalyst with higher Ni loading produces more hydrogen; this is related with more Ni active sites in the surface of the catalyst for methane decomposition.

3.3. Carbon Nanotube Formation

The formation of carbon nanotubes was studied by using Raman spectroscopy and electron transmission microscope. **Figure 5** shows a Raman spectrum of the 30 wt% Ni/MCM-41 catalyst after 500 min of reaction. Two bands around 1576 cm^{-1} and 1325 cm^{-1} are observed. The peak around 1576 cm^{-1} corresponds to G band of the graphitic carbon arising from the C-C stretching vibration; the peak around 1325 cm^{-1} is assigned to D band, corresponding to amorphous carbon or disorder structure and lattice defects in the microcrystalline carbon [12]. Raman spectrum indicates that two kinds of carbon were formed in the catalysts.

Figure 6 shows the TEM micrographs of the spent catalysts. Many CNTs with thick (multiwall) layers are clearly observed (**Figure 6(a)**). It is found that CNTs mainly grew with a tip-growth mode in which CNTs grow with Ni particle on its tip. This can be explained by the interaction degree between the Ni particles and the MCM-41 support [13]. In the present work, the Ni is introduced onto the surface of the support by impregnation, and therefore, Ni particles are mainly loaded on the surface but are not embedded or anchored inside the support, thus interaction between the Ni particles and the support is weak, which is in favour of the formation of carbon nanotube through the tip-growth mode, prevent the Ni particles from carbon encapsulation, and thus the

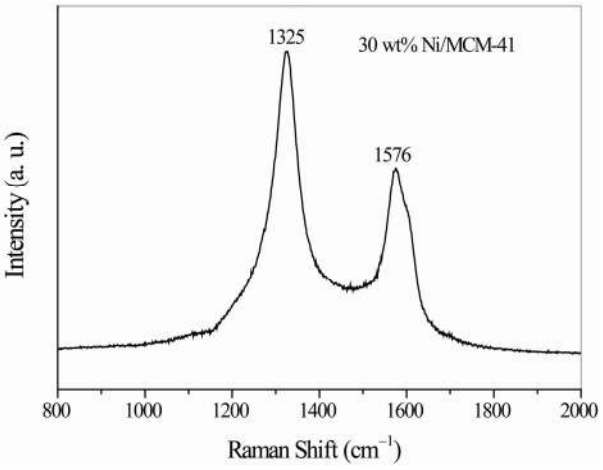

Figure 5. A Raman spectrum of 30%Ni/MCM-41 spent catalyst after 500 min of reaction.

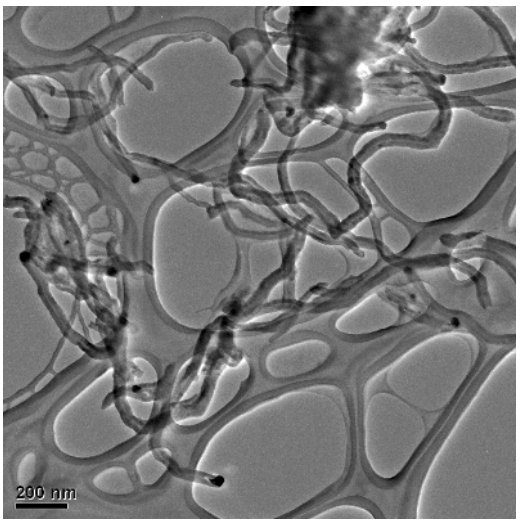

(a)

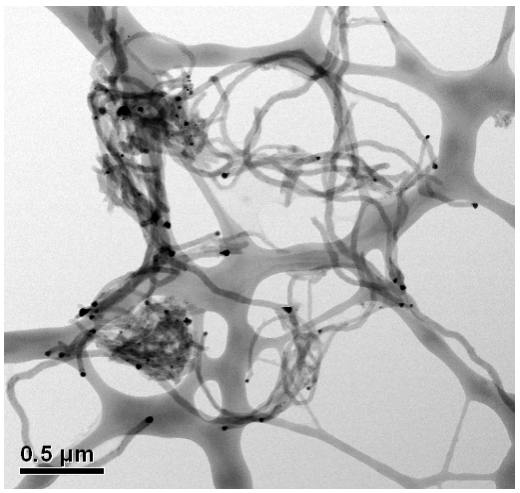

(b)

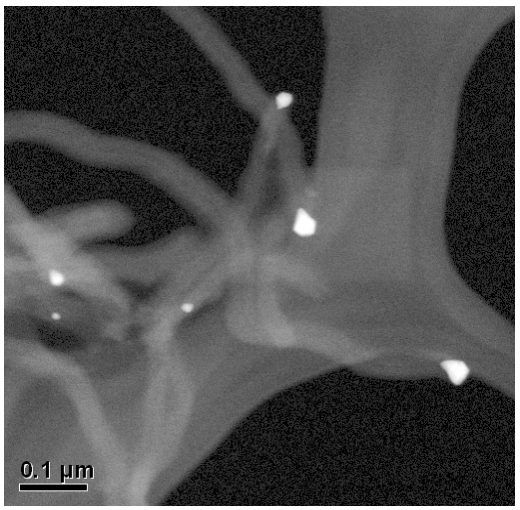

(c)

Figure 6. TEM micrographs of the 30 wt% Ni/MCM-41 catalyst after 500 min reaction.

catalyst remains a long lifetime. The diameter of CNTs has a close relation with the Ni particle size; large Ni particles lead to formation of CNTs with big diameter (**Figure 6(b)**). As a result, the inner diameter of the CNTs is largely determined by the diameter of the Ni particle. It is also observed that almost all of the CNTs, no matter whether they have thin or thick tube walls, are curved in certain degree (**Figures 6(a)** and **(b)**).

On the fresh Ni/MCM-41 catalysts, most of the Ni particles have a shape as pseudo-sphere (**Figure 2**). However, after the reaction, the Ni particle shows a shape diamond-like with a tail inserting into the carbon nanotube (**Figure 6(c)**). It is known that the melting point of metallic Ni is around 1452˚C, Ni particle may change its shape only at a temperature above its Tamman point T_m = 726˚C. Under the present reaction condition, the reaction temperature is 550˚C. It seems impossible for Ni particle to alter its shape. It is reported that on a spent Ni/SiO_2 catalyst, Ni carbide (Ni_3C) is formed [14]. Ni_3C is unstable and it can be decomposed into nickel and graphitic carbon at a relative low temperature, *i.e.*, 400˚C. It is also proven that carbon atoms produced from CH_4 decomposition over the Ni based catalysts can form Ni_xC_y solid solution as intermediate [15], at such condition, C atoms are able to move within the bulk of Ni particles and are then they are released from the Ni_xC_y solid solution to form nanotubes at the interface of the Ni particle and support. Because methane decomposition is an exothermic reaction (ΔH = 75 kJ/mol), the temperature around Ni particle surface is, therefore, at somewhat overheat state, with respect to its surrounding temperature. As a result, the Ni-C system may transfer into a quasi-liquid state at a reaction temperature even lower than the Tamman temperature of Ni; this provides the possibility for Ni changing its shape. It is also noted that a gradient of carbide concentration in the Ni particles during the reaction leads to pressure built up at the interface of Ni and support. When the graphitic layers are initially formed in parallel to the Ni crystal surface, carbon nanotube growth along the Ni crystal surface may drive the Ni particles to be squeezed out, changing Ni shape from pseudo-sphere to diamond-like.

4. Conclusion

The present work confirms that simultaneous production of hydrogen and CNTs can be realized in a single reaction of methane catalytic decomposition by using Ni/MCM-41 as catalyst. The Ni/MCM-41 catalysts exhibit high catalytic stability during 500 min of reaction. The formed CNTs have 20 - 50 nm in diameters and a few micrometers in length, depending on the reaction condition. Large Ni particles usually favour the formation of CNTs with big diameter. During the reaction, the shape of Ni particles changes from pseudo-sphere to diamond-like. All the CNTs consist of multiple layer walls and are curved in certain degree. The CNTs formation may grow with a tip-growth mode due to the weak interaction between Ni and MCM-41 support.

5. Acknowledgements

The authors would like to thank Mr. L. A. Moreno, Dr. J. Alberto Andraca Adame, and Dr. C. Angeles for their technical assistance.

REFERENCES

[1] L. Barretoa, A. Makihira and K. Riahi, "The Hydrogen Economy in the 21st Century: A Sutainable Development Scenario," *International Journal of Hydrogen Energy*, Vol. 28, No. 3, 2003, pp. 276-284.

[2] P. Tomczyk, "Fundamental Aspects of the Hydrogen Economy," *World Futures*: *The Journal of Global Education*, Vol. 65, No. 5-6, 2009, pp. 427-435. doi:10.1080/02604020903021818

[3] J. D. Holladay, "An Overview of Hydrogen Production Technologies," *Catalysis Today*, Vol. 139, No. 4, 2009, pp. 244-260. doi:10.1016/j.cattod.2008.08.039

[4] Y. Li, D. Li and D. Wang, "Methane Decomposition to CO_x-Free Hydrogen and Nano-Carbon Materials on Group 8-10 Base Metal Catalysts: A Review," *Catalysis Today*, Vol. 162, No. 1, 2011, pp. 1-46. doi:10.1016/j.cattod.2010.12.042

[5] K. P. De Jong and J. W. Geus "Carbon Nanofibers: Catalysis Synthesis and Applications," *Catalysis Review*: *Science & Technology*, Vol. 42, No. 2, 2000, pp. 481-510.

[6] P. J. F. Harris, "Carbon Nanotubes and Related Structures: New Materials for the Twenty-First Century," Cambridge University Press, Cambridge, 2003.

[7] M. S. Rahammad, E. Croiset and R. R. Hudgins, "Catalytic Decomposition of Methane for Hydrogen Production," *Topics in Catalysis*, Vol. 37, No. 2-4, 2006, pp. 137-145. doi:10.1007/s11244-006-0015-8

[8] M. A. Ermakova, D. Y. Ermakov, A. L. Chuvilin and G. G. Kuvshinov, "Decomposition of Methane over Iron Catalysts at the Range of Moderate Temperatures: The Influence of Structure of the Catalytic Systems and the Reaction Conditions on the Yield of Carbon and Morphology of Carbon Filaments," *Journal of Catalysis*, Vol. 201, No. 2, 2001, pp. 183-197. doi:10.1006/jcat.2001.3243

[9] J. S. Beck, J. C. Vartuli, W. J. Roth, M. E. Leonowics, C. T. Kresge, K. D. Schmitt, C. T.-W. Chu, D. H. Olson, E. W. Sheppard, S. B. McCullen, J. B. Higgins and J. L. Schlenker, "A New Family of Mesopoous Molecular Sieves Prepared with Liquid Crystal Template," *Journal of the American Chemical Society*, Vol. 114, No. 27, 1992, pp. 10834-10843. doi:10.1006/jcat.2001.3243

[10] A. Sayari, M. Jaroniec and T. J. Pinnavaia, "Studies in Surface Science and Catalysis. Vol. 129: Nanoporous Materials II," Elsevier Science, Amsterdam, 2000.

[11] H. C. Liu, H. Wang, J. H. Shen, Y. Sun and Z. M. Liu,

"Preparation, Characterization and Activities of Nano-Sized Ni/SBA-15 Catalyst for Producing COx-Free Hydrocarbon from Ammonia," *Applied Catalysis A*: *General*, Vol. 337, No. 2, 2008, pp. 138-147.

[12] A. Jorio, M. A. Pimenta, A. G. Souza Pilho, R. Satio, G. Dresselhaus and M. S. Dresselhaus, "Characterizing Carbon Nanotube Samples with Resonance Raman Scattering," *New Journal of Physics*, Vol. 5, No. 1, 2003, p. 139.

[13] E. Laouroux, P. Serp and P. Kalck, "Catalytic Routes toward Single Wall CNTs," *Catalysis Review*: *Science & Technology*, Vol. 49, No. 3, 2007, pp. 341-405.

[14] T. V. Choudhary, C. Sivadinarayana, C. C. Chusuei, A. Klinghoffer and D. W. Goodman "Hydrogen Production via Catalytic Decomposition of Methane," *Journal of Catalysis*, Vol. 199, No. 1, 2001, pp. 9-18. doi:10.1006/jcat.2000.3142

[15] P. L. Hansen, S. Helveg and A. K. Dayte, "Atomic-Scale Imaging of Supported Metals Nanocluster Catalysts in the Working State," *Advanced Catalyst*, Vol. 50, 2006, pp. 77-95. doi:10.1016/S0360-0564(06)50002-1

